Preferential Orientation of Lamellar Microdomains Induced by Uniaxial Stretching of Cross-Linked Polystyrene-*block*-polybutadiene-*block*-polystyrene Triblock Copolymer

Shinichi Sakurai,*,† Sakae Aida,† Shigeru Okamoto,‡ Takashi Ono,§ Kimio Imaizumi,§,|| and Shunji Nomura†

Department of Polymer Science and Engineering, Kyoto Institute of Technology, Matsugasaki, Sakyo-ku, Kyoto 606-8585, Japan; Department of Material Science and Engineering, Nagoya Institute of Technology, Gokiso-cho, Showa-ku, Nagoya 466-8555, Japan; Plastics Development and Technology Center, Asahi Chemical Industry Co., Ltd., Yako, Kawasaki-ku, Kawasaki 210-0863, Japan; and Department of Material Science and Engineering, Shibaura Institute of Technology, Shibaura, Minato-ku, Tokyo 108-8548, Japan

Received December 13, 2000

ABSTRACT: We report an experimental result for a lamellar orientation in cross-linked polystyrene-*block*-polybutadiene-*block*-polystyrene (SBS) triblock copolymer that was uniaxially drawn at 130 °C (above the glass transition temperature of polystyrene; $T_{g(PS)}$). The lamellar orientation was examined using two-dimensional small-angle X-ray scattering (2d-SAXS) experiments. It was revealed that the lamellar normal preferentially oriented perpendicular to the stretching direction such that the microdomain interface between polystyrene and polybutadiene lamellae is more or less parallel to the stretching direction, where the lamellar normal denotes the direction normal to the lamellar interface. On the other hand, a herringbone structure was induced by the uniaxial stretching for a sample drawn at room temperature (below $T_{g(PS)}$) without the lamellar orientation. Therefore, it is concluded that the strain-induced orientation of lamellae can be only attained above $T_{g(PS)}$ and that the uniaxial stretching above $T_{g(PS)}$ was found to be an effective way to induce the preferential orientation of lamellae. The lamellar orientation was found to be improved by the thermal annealing at a stretched state and more by increasing the extent of the stretching, as well as cross-linking density.

Introduction

Block copolymers undergo microphase separation and form well-ordered structures, such as spheres, cylinders, gyroid, and lamellae.[1] It is empirically known that the macroscopic physical properties of the block copolymers are correlated with the microdomain structures. In this regard, the preferential orientation of the microdomains may be the key for introduction of anisotropy of macroscopic properties. For lamellar microdomains, orientation under extensional flow or dynamic shear flow has been extensively studied.[2−9] Under extensional flow, a preferential orientation can be attained with appropriate experimental conditions.[2−4] On the other hand, under the dynamic (oscillatory) shear flow not only *parallel* orientation but also *perpendicular* orientation are observed, depending upon the deformation frequency and amplitude.[9] A *biaxial* orientation is even found under the oscillatory shear flow with a large-amplitude and high-frequency deformation.[8]

Recently Panyukov and Rubinstein[11] have demonstrated theoretically the eligibility of tensile strain for the preferential orientation of lamellar microdomains. To experimentally examine, we should at least stretch the sample at temperatures above the glass transition temperature of the constituent block chains. Thus, chemical cross-links are required. In our previous study,[12,13] we conducted chemical cross-linking of the polybutadiene (PB) chains in the disordered state of polystyrene-*block*-polybutadiene-*block*-polystyrene (SBS) triblock copolymers, which was followed by microphase separation and further uniaxial stretching above the glass transition temperature of the polystyrene (PS), $T_{g(PS)}$. Although the morphology of the microdomains is lamellar in the virgin sample, ill-ordered bicontinuous microdomain structure was formed in the as-cross-linked sample because the lamellar formation may be kinetically prevented by the chemical cross-links in the PB chains.[12] Upon the uniaxial stretching of this sample, an embryonic region of lamellae was formed, but no preferential lamellar orientation was attained. In the present study, we conducted the chemical cross-linking in the ordered state, namely, cross-linking of the PB chains in the lamellar microdomain space. And the eligibility of the uniaxial stretching for a preferential orientation was studied using two-dimensional small-angle X-ray scattering (2d-SAXS) technique.

Experimental Section

The SBS triblock copolymer used in this study has the following molecular characteristics; $M_n = 6.31 \times 10^4$, $M_w/M_n = 1.15$, and $\phi_{PS} = 0.56$ where M_n and M_w denote the number-average and the weight-average molecular weights, respectively, and ϕ_{PS} is the volume fraction of the PS blocks. The concentration of cross-linker (c_X) was in the range of $0.5 \le c_X \le 4.0$ wt %. The SBS sample and the cross-linker, which is 1,1-bis(*tert*-butylperoxy)-3,3,5-trimethylcyclohexane, was dissolved in toluene (the polymer concentration was ca. 5 wt %). Then the solution was poured into a flat Petri dish to allow gradual evaporation of the solvent. After complete evaporation for ca. 7 days at room temperature, an as-cast film was obtained with ca. 0.5 mm thickness. To activate the cross-

* To whom all correspondence should be addressed. E-mail: shin@ipc.kit.ac.jp.
† Kyoto Institute of Technology.
‡ Nagoya Institute of Technology.
§ Asahi Chemical Industry Co., Ltd.
|| Shibaura Institute of Technology.

10.1021/ma002123+ CCC: $20.00
Published on Web 04/27/2001

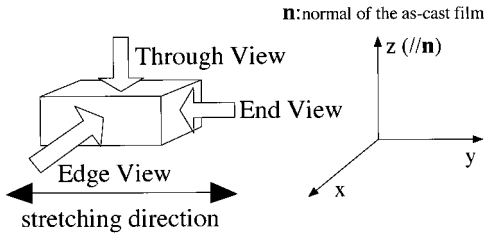

Figure 1. Schematic drawing of the experimental Cartesian axes with respect to the uniaxial stretching direction. Here, the *y*-axis is chosen to be parallel to the stretching direction, and the *z*-axis is parallel to the normal of a sample film.

linker, which cross-links only the PB chains, the as-cast sample was annealed thermally at 150 °C for 100 min.[12,13]

We conducted uniaxial stretching at 130 °C for the SBS samples of which PB lamellae were cross-linked chemically by the cross-linker. Since the sample was broken when the stretched sample was exposed to the long-term annealing at 130 °C, we conducted the following experimental procedure. First, the sample was stretched out in the heating blocks under the atmospheric condition (no nitrogen substitution at all). The uniaxial draw ratio ϵ ($\epsilon = l/l_0$, where l and l_0 denote lengths of the film at stretched and unstretched state, respectively) is in a range of $2 \leq \epsilon \leq 6$, and the draw speed $\dot{\varepsilon}$ was about 0.09 s^{-1}. Then the sample was quenched to 0 °C in the ice/water mixture in order to lock the sample at a stretched state below $T_{g(PS)}$. After the sample was removed from a drawing device, it was sandwiched by a two pieces of flat glass plate. Note that the glass plate enabled us to prevent the drawn sample from relaxing or suffering breaks during the thermal annealing at 130 °C for a given duration.

To quantify the degree of ordering and the degree of the lamellar orientation, we conducted 2d-SAXS experiments, which were mainly performed at the BL-15A (SAXS beamline) in the Photon Factory of the Research Organization for High Energy Accelerator, Tsukuba, Japan. The imaging plate (250 × 200 mm^2), of which the actual pixel size is 100 × 100 μm^2, was used as a two-dimensional detector. The typical exposure time was in the range 1−4 s. BAS2000 (Fuji Photo Film Co., Ltd.) was used for development of exposed 2d-SAXS images. The 2d-SAXS patterns were further converted to one-dimensional profile by conducting so-called sector averaging. No further correction such as a background subtraction was made on the 1d- and 2d-SAXS results.

The schematic drawings in Figure 1 indicate the experimental Cartesian axes with respect to the stretching direction. Here the *y*-axis is chosen to be parallel to the stretching direction and the *z*-axis is parallel to the normal of a sample film. For the uniaxially drawn sample, three different views, i.e., through, edge, and end views, can be identified. Note that the through view SAXS pattern is recorded on the *x*−*y* plane by sending the incident X-ray beam from the *z*-direction. The edge view SAXS pattern is recorded on the *y*−*z* plane with the incident beam from the *x*-direction, and the end view SAXS pattern is on the *x*−*z* plane with the incident beam from the *y*-direction.

Transmission electron micrographs were taken with JEM-2010 (JEOL Ltd., Japan) operated at 100 kV acceleration voltage. The samples were embedded in cured epoxy resin and then ultramicrotomed with ULTRACUT S (REICHERT-NISSEI Co. Ltd.) at cryogenic temperature (−80 °C) using the FC-S cryogenic system (REICHERT-NISSEI Co. Ltd.). The thickness of the ultramicrotomed specimens was about 65 nm. The specimens were stained with a vapor of 2% aqueous solution of osmium tetraoxide (OsO_4) for 60 min and then subjected to the TEM observation.

Results and Discussion

Figure 2 shows the 2d-SAXS pattern (gray scale for the logarithmic intensities) for the as-cast film at unstretched state (parts a and b), and at stretched state

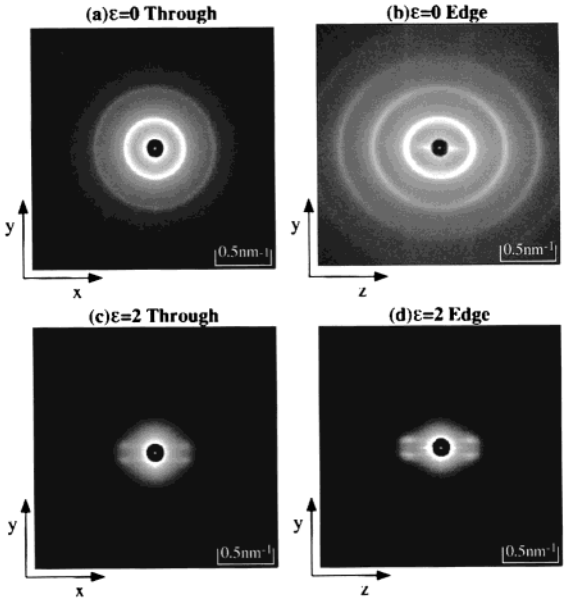

Figure 2. 2d-SAXS patterns (gray scale for the logarithmic intensity) for an as-cast film in the unstretched state, (a) through view and (b) edge view, and for a stretched film, (c) through view and (d) edge view (stretched at room temperature with $\epsilon = 2.0$, where ϵ denotes the draw ratio as defined by $\epsilon = l/l_0$, with l and l_0 being lengths of the film in the stretched state and the unstretched state, respectively).

with $\epsilon = 2$ (parts c and d). In the pattern for the as-cast unstretched film, isotropic circular rings were observed. The intensity is almost independent of the azimuthal angle. These rings are ascribed to diffraction resulted from one-dimensionally alternating lamellar microdomains because the q values for the diffraction rings can relatively be assigned to 1:2:3..., where q denotes the magnitude of the scattering vector as defined by $q = (4\pi/\lambda) \sin(\theta/2)$ with λ and θ being the wavelength of the X-ray beam ($\lambda = 0.1504$ nm) and the scattering angle, respectively. It is needless to note that the isotropic 2d-SAXS patterns in through and edge views indicate random orientation of grains in which lamellar microdomains are regularly ordered. When the edge and through views are compared, however, the regularity of ordered lamellae is found to be much superior in the edge view than in the through view, because up to fourth-order diffraction rings can be identified in the edge view (mainly in the *z*-direction) whereas up to second-order peaks are observed in the through view. This result in turn indicates that the lamellar structures have a tendency to order preferentially with respect to the substrate- and air-contacting surfaces of the as-cast film, such that the microdomain interface between PS and PB lamellae is more or less parallel to the surfaces. Such an effect of the solution casting was reported more than 20 years ago.[14] The edge view SAXS pattern was skewed (elongated in the *z*-direction, i.e., the first-order peaks appear at $q_y^* = 0.261$ nm^{-1} and $q_z^* = 0.297$ nm^{-1}). The lamellae, of which interfaces orient parallel to the substrate- and air-contacting surfaces, are expected to be compressed along the direction normal to the as-cast film.[15] On the other hand, the lamellae, of which interfaces orient perpendicularly to the substrate- and air-contacting surfaces of the as-cast film, are not compressed. Therefore, the repeat distance is larger so that the position of the first-order peak in the *x*- and *y*-directions is smaller than that in the *z*-direction ($q_x^* \approx q_y^* < q_z^*$). This fact results in the isotropic and

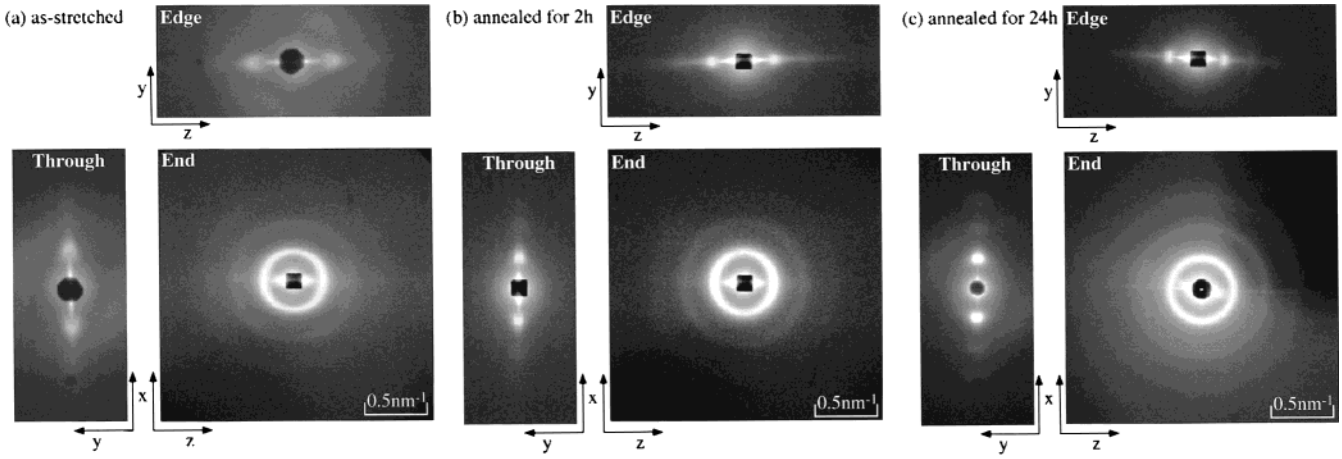

Figure 3. 2d-SAXS pattern (gray scale for the logarithmic intensity) for a cross-linked film ($c_x = 4.0$ wt %) under stretched state with $\epsilon = 5.0$: (a) as-stretched, (b) annealed at 130 °C for 2 h, and (c) annealed at 130 °C for 24 h.

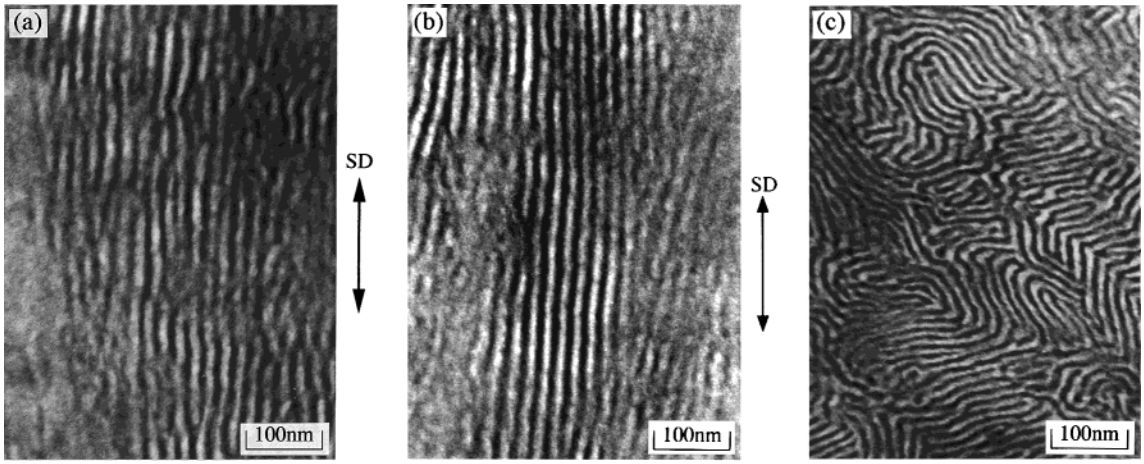

Figure 4. Transmission electron micrographs for (a) through, (b) edge, and (c) end views of a stretched sample that was further annealed at 130 °C for 24 h under a stretched state with $\epsilon = 5.0$. The concentration of the cross-linker was 4.0 wt %. The dark regions are ascribed to PB microdomains stained with OsO_4, and the bright ones are unstained PS microdomains.

anisotropic 2d-SAXS patterns in the through and edge views, respectively. The higher intensities at diffraction peaks in the *z*-direction as compared to that in the *y*-direction was also detected in the edge view (Figure 2a; $I(q_y) < I(q_z)$). This result is also ascribed to the preferential lamellar orientation in the as-cast sample mentioned above.

Upon uniaxial stretching of the as-cast film of lamellar forming block copolymers at room temperature, it is well-known that the lamellar structure changes into a herringbone structure.[10] As a result, the 2d-SAXS pattern drastically changes into that shown in Figure 2, parts c and d. Here, the characteristic four streaks perpendicular to the stretching direction were observed, being ascribed to the herringbone structure. At room temperature, the PS microdomains are in a glassy state so that they are broken and segmented under the load, whereas the rubbery PB microdomains can deform elastically. Hence, putting the one-dimensional strain onto the alternating lamellar grain results in the herringbone structure.

On the contrary, the structural change caused by the uniaxial stretching at temperatures above $T_{g(PS)}$ was expected to be greatly different such that we can preferentially orient the lamellar structures with respect to the stretching direction. To draw the sample, chemically cross-linking the PB block chains is eligible. In Figure 3, typical examples of the 2d-SAXS pattern being resulted from high and preferential orientation of the lamellar structures are demonstrated for the sample cross-linked with $c_X = 4.0$ wt % which was annealed at 130 °C for 0, 2, and 24 h under the stretched state with $\epsilon = 5.0$. Not only in the edge view, but also in the through view, the diffraction peaks concentrated their intensities on the *x*- and *z*-directions which are perpendicular to the stretching (*y*) direction. As a result, the 2d-SAXS pattern becomes spotty. On the other hand, the pattern is still isotropic and circular in the end view. From these results, it is concluded that the lamellar microdomains preferentially orient along the stretching direction while the orientation is axially symmetric with respect to it. Namely, the lamellar normal preferentially orients perpendicular to the stretching direction. Here the lamellar normal denotes the direction normal to the interface between PS and PB lamellae. Note that streaks resulted from the total reflection of the incident X-ray beam by the surface of the sample film.

Figure 4, parts a−c, shows the transmission electron micrographs in through, edge, and end views, respectively, for the stretched sample that was further annealed at 130 °C for 24 h under a stretched state with $\epsilon = 5.0$. The dark regions are ascribed to the PB microdomains stained with OsO_4, and the bright ones are the unstained PS microdomains. The preferential orientation along the stretching (*y*) direction can be seen

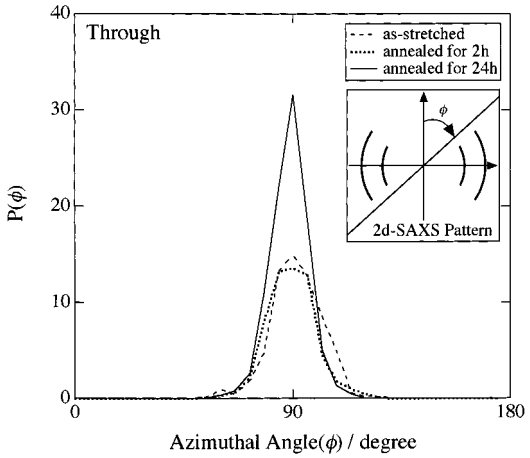

Figure 5. Apparent normalized orientation distribution function, $P(\phi)$, where ϕ denotes the azimuthal angle that is defined as the angle from the principal direction (meridian), perpendicular to which the diffraction spots appeared. These results were obtained from the 2d-SAXS pattern for the through view (as-stretched, and annealed at 130 °C for 2 and 24 h for the sample cross-linked with $c_x = 4.0$ wt %).

in Figure 4, parts a and b, whereas axisymmetric lamellar orientation is more likely seen in Figure 4c. These results are in accord with the 2d-SAXS results. Note here that the feature observed in Figure 4, parts a−c, was discernible in a considerably wide area of the respective TEM image.

For quantitative discussion of the lamellar orientation, we will show the scattering intensity as a function of the azimuthal angle, ϕ, where the azimuthal angle is defined as the angle from the principal direction (meridian), perpendicular to which the diffraction spots appeared, namely perpendicular to the lamellar normal. For the sake of more convenience, the normalized orientation distribution function, $P(\phi)$, is introduced. It is defined by

$$P(\phi) = I(q^*,\phi)\, q^{*2} / \int_0^{\pi} I(q^*,\phi)\, q^{*2} \sin\phi \, d\phi \qquad (1)$$

where $I(q^*)$ is the scattering intensity at the first-order peak position. Figure 5 shows change of $P(\phi)$ as a function of the annealing time for the through view. Upon 2 h of annealing, little change was discernible. On the other hand, after 24 h of annealing, a remarkable increase in $P(\phi)$ at $\phi = 90°$ was detected. Similar facts were observed for the edge view, while $P(\phi)$ is almost uniform with $P(\phi) = 0.5$ for the end view SAXS pattern. These results suggest that the axisymmetric lamellar orientation is readily induced by the uniaxial stretching at 130 °C and it proceeds further by the annealing up to 24 h. The second-order orientation factor, F_2, is evaluated for the sake of more quantitative discussion

$$F_2 = C^{-1}\,[3\langle\cos^2\phi\rangle - 1]/2 \qquad (2)$$

where C is a conversion constant from the orientation of a lamellar normal to that of a lamellar interface with respect to the stretching direction, and is given by

$$C = (3\cos^2\Phi - 1)/2 \qquad (3)$$

Φ denotes the angle of the lamellar normal to the lamellar interface and indeed $\Phi = 90°$; hence, $C = -1/2$. Thus, the defined second-order orientation factor, F_2,

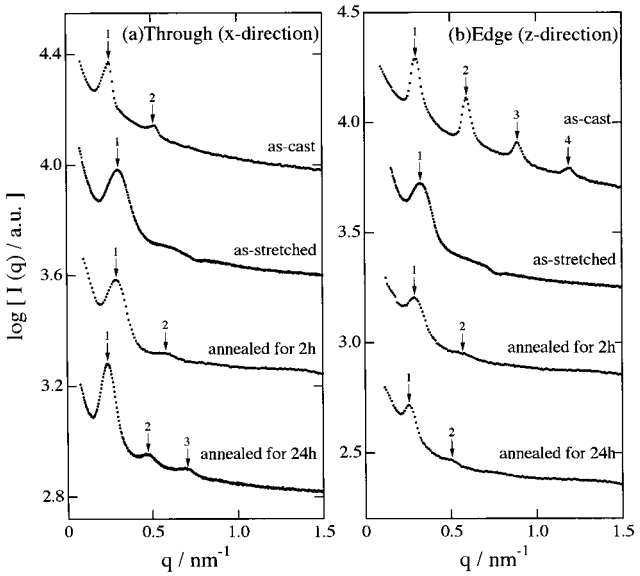

Figure 6. 1d-SAXS profiles converted from the 2d-SAXS patterns by conducting the sector averaging over the azimuthal angle $\phi = 90 \pm 5°$ and $\phi = 270 \pm 5°$ for as-cast, as-stretched, and annealed at 130 °C for 2 and 24 h for the sample cross-linked with $c_x = 4.0$ wt %: (a) through view (**q**//*x*-direction) and (b) edge view (**q**//*z*-direction).

characterizes quantitatively the orientation of the lamellar interface with respect to the stretching direction. In eq 2, $\langle\cos^2\phi\rangle$ denotes the average of $\cos^2\phi$, which is given by

$$\langle\cos^2\phi\rangle = \int_0^{\pi} \cos^2\phi\, P(\phi) \sin\phi \, d\phi \qquad (4)$$

Variations of F_2 with the annealing time will be discussed later.

Conducting the sector averaging over the azimuthal angles, $\phi = 90 \pm 5°$ and $\phi = 270 \pm 5°$, the 2d-SAXS patterns were converted to one-dimensional SAXS profiles that are displayed in Figure 6. Here the profiles were vertically shifted to avoid their overlaps. In the edge view (*z*-direction) for the as-cast film, diffraction peaks appeared up to the fourth-order, suggesting well-ordered microdomain structures in a grain, although the orientation of grains is not preferential with respect to the *z*-direction. Upon uniaxial stretching, both in the *x*-direction (through view) and in the *z*-direction (edge view), the first-order peak was significantly broadened with a shift toward a higher q range. With an increase in the annealing time, the first-order peak became sharper with a shift toward lower q range. Moreover, higher-order peaks appeared gradually as the thermal annealing at 130 °C were prolonged. To discuss the change in the degree of ordering of the lamellar structures with the annealing time, change in the width of the first-order peak (hwhm; the half-width at the half-maximum) was examined. The repeating distance of alternating lamellae is also calculated from the position of the diffraction peak by $D = 2\pi/q^*$ where q^* denotes the q value of the first-order diffraction peak.

The values of F_2, hwhm, and D were plotted as a function of the annealing time for the through and edge views in Figure 7, parts a−c, respectively. Note that the values of F_2 and hwhm were evaluated based on the data for the first-order peak. In Figure 7, parts b and c, the broken lines indicate the values for the as-cross-linked film in the through view (*x*-direction). It was

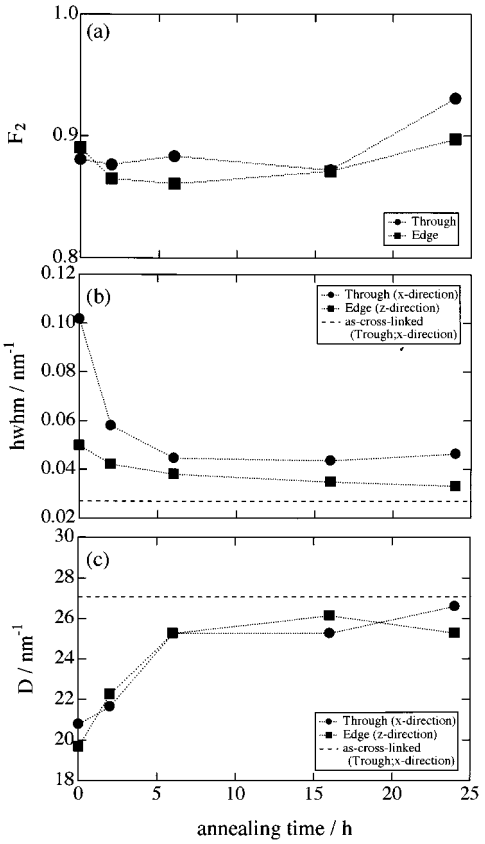

Figure 7. Changes in the orientation factor (F_2), the peak width of the first-order peak (hwhm), and the lamellar repeating period (D) as a function of the annealing time were displayed for the sample cross-linked with $c_x = 4.0$ wt %. Here F_2 was evaluated from the 2d-SAXS pattern using the first-order peak intensity and D was calculated from the position of the first-order peak. Filled circles are for the through view (x-direction) and filled squares are for the edge view (z-direction). In parts b and c, the broken line indicates the level for the as-cross-linked film, which was evaluated from its through view (z-direction).

found that the value of F_2 significantly increased from 0 to 0.88 upon uniaxial stretching (at the zero-hour annealing) and then more or less increased with an increase of the annealing time. Eventually, the value reached as high as 0.93 after 24 h of annealing. The value of hwhm for the first-order lattice peak significantly increased upon the uniaxial stretching (at the zero-hour annealing) and then decreased rapidly with an increase of the annealing time both in the through and edge views. The value eventually leveled off to the values slightly larger than that for the as-cross-linked unstretched sample. It is noteworthy that at the zero-hour annealing the value is much larger in the through view.

The lamellar repeat period, D, is found to decrease rapidly upon the uniaxial stretching because the value of D at the zero-annealing time were smaller than that of D obtained for the as-cross-linked unstretched sample. Then, it increased with the annealing time up to about 6 h. Note, however, that the value of D eventually reached the similar value for the as-cross-linked unstretched sample. On the basis of these results, the change in the lamellar structure upon the uniaxial stretching can be considered as follows. Upon the uniaxial stretching, the lamellae in the x- and z-directions (both are perpendicular to the stretching direction) are compressed, and the regularity of the

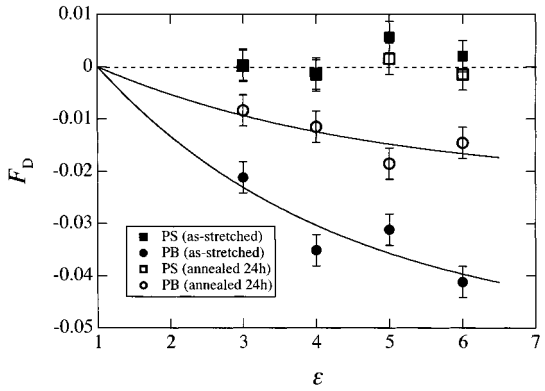

Figure 8. Dichroic ratio orientation factor, F_D, as a function of the draw ratio (ϵ) for PS and PB chains. The results for the sample cross-linked with $c_x = 4.0$ wt % are shown.

repeating lamellae becomes worse. By thermal annealing of the stretched sample, the lamellae in the x- and z-directions thickened to recover the original thickness even though the sample was annealed at the stretched state. In the meantime, the regularity of the lamellae can proceed without degrading the lamellar orientation, and even the orientation more or less proceeds. Thus, the uniaxial stretching above $T_{g(PS)}$ was found to be an effective way to induce the lamellar orientation. Further thermal annealing results in the better ordering and more or less higher orientation of the lamellar structures.

Upon the uniaxial stretching above $T_{g(PS)}$, the cross-linked PB chains should be oriented along the stretching direction. To check this conjecture, the molecular orientation was examined by the Fourier transform infrared spectroscopic measurements. According to the method reported,[16] the value of the dichroic ratio orientation factor, F_D, were obtained for PB from the dichroic ratio of the absorption band at 966 cm^{-1}, which is ascribed to an out-of-plane CH bending mode in *trans*-1,4-PB. The values of F_D were also evaluated for PS using the absorption band at 1493 cm^{-1}. The results for the sample cross-linked with $c_x = 4.0$ wt % are shown in Figure 8. Since the transition moment of the out-of-plane CH bending mode for PB is almost perpendicular to the main chain, negative values of F_D indicate parallel orientation of the PB chain molecules along the stretching direction. A similar argument can be made for F_D of PS, though the band at 1493 cm^{-1} is not so sensitive to the orientation.[16] As is expected, it is seen in Figure 8 that the PB chains orient parallel to the stretching direction and that the orientation proceeds monotonically with the stretching. On the other hand, no appreciable orientation was detected for the PS chains. This result indicates that the PS lamellar microdomains flow upon the uniaxial stretching above $T_{g(PS)}$ and that orientation of the un-cross-linked PS chains resulted from the extensional flow, if any, has been already relaxed. From Figure 8, it further turned out that the orientation of the PB chains in the as-stretched sample was relaxed to some extent by thermal annealing for 24 h. As a consequence, the chain dimension of PB perpendicular to the stretching direction should be increased, which in turn should result in an increase in D because the lamellar repeating direction is perpendicular to the lamellar interface that is approximately parallel to the stretching direction in the stretched samples. This scenario can explain the increase in D by the thermal annealing in Figure 7c.

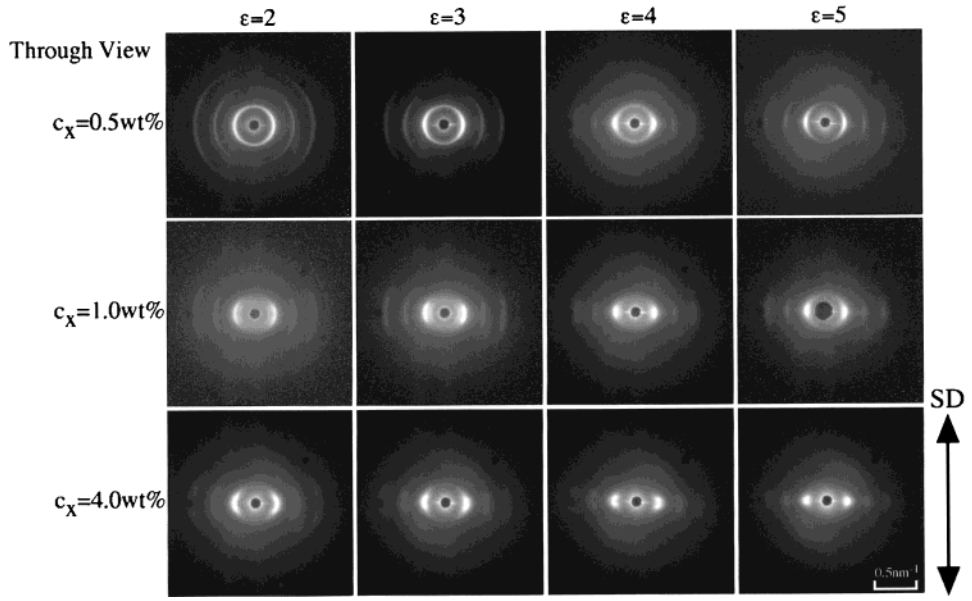

Figure 9. 2d-SAXS patterns (gray scale for the logarithmic intensity for the through view) obtained for films cross-linked with various concentrations of the cross-linker (c_x). The films were thermally annealed at 130 °C for 24 h under a stretched state with various values of the draw ratio (ϵ).

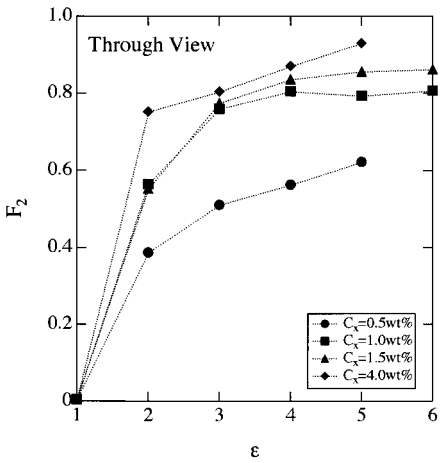

Figure 10. Variation of the orientation factor, F_2, as a function of ϵ, for films cross-linked with various concentrations of the cross-linker (c_x).

Finally, we discuss effects of the cross-linking density and the extent of stretching. Figure 9 displays changes of 2d-SAXS patterns (distribution of the logarithmic scattering intensities for through view geometry) as functions of c_x and ϵ. For slightly cross-linked and stretched sample ($c_x = 0.5$ wt % and $\epsilon = 2.0$), all of the diffraction peaks exhibit wide arcs. It is remarkable that with increasing c_x and ϵ the diffraction peaks concentrate their intensities on the equator that is perpendicular to the stretching direction. At the highest c_x and ϵ ($c_x = 4.0$ wt % and $\epsilon = 5.0$), the diffraction arcs evolved into spots. Comparison of those 2d-SAXS patterns definitely demonstrates improvement of the lamellar orientation. It is more quantitatively confirmed in Figure 10 where the variations of the orientation factor F_2 with elongation are shown for various values of c_x. Note that its highest value is as large as 0.93.

Conclusion

Lamellar orientation by uniaxial stretching of cross-linked SBS triblock copolymer was examined by the 2d-SAXS technique. Above $T_{g(PS)}$ at $\epsilon = 5.0$, highly oriented lamellar structures were confirmed for $c_x = 4.0$ wt %. The lamellar normal preferentially oriented perpendicular to the stretching direction. Thermal annealing of the stretched sample results in the better ordering and more or less higher orientation of the lamellar structures. It was also found that the lamellar orientation was improved with increasing the extent of stretching as well as cross-linking density.

Acknowledgment. This work is supported in part by a Grant-in-Aid from the Japanese Ministry of Education, Culture, Science, and Sport (11750781), granted to S.S. A research grant from the Mitsubishi Petrochemical Foundation to S.S. is also gratefully acknowledged. We thank Dr. Panyukov for fruitful discussions. The SAXS experiments were mainly performed in the Photon Factory of the Research Organization for High Energy Accelerator, Tsukuba, Japan, with approval number 98G128.

References and Notes

(1) Sakurai, S. *Trends Polym. Sci.* **1995**, *3*, 90.
(2) Keller, A.; Pedemonte, E.; Willmouth, F. M. *Kolloid Z. Z. Polym.* **1970**, *238*, 2329; *Nature* **1970**, *225*, 538.
(3) Hadziioannou, G.; Mathis, A.; Skoulios, A. *Colloid Polym. Sci.* **1979**, *257*, 136. Hadziioannou, G.; Picot, C.; Skoulios, A.; Ionescu, M.-L.; Mathis, A.; Duplessix, R.; Gallot, Y.; Lingelser, J.-P. *Macromolecules* **1982**, *15*, 263.
(4) Scott, D. B.; Waddon, A. J.; Lin, Y.-G.; Karasz, F. E.; Winter, H. H. *Macromolecules* **1992**, *25*, 4175.
(5) Koppi, K. A.; Tirell, M.; Bates, F. S.; Almdal, K.; Colby, R. H. *J. Phys. II (Fr.)* **1992**, *2*, 1941. Almdal, K.; Koppi, K. A.; Bates, F. S.; Mortensen, K. *Macromolecules* **1992**, *25*, 1743.
(6) Winey, K. I.; Patel, S. S.; Larson, R. G.; Watanabe, H. *Macromolecules* **1993**, *26*, 2542, 4373.
(7) Morrison, F. A.; Mays, J. W.; Muthukumar, M.; Nakatani, A. I.; Han, C. C. *Macromolecules* **1993**, *26*, 5271.
(8) Okamoto, S.; Saijo, K.; Hashimoto, T. *Macromolecules* **1994**, *27*, 5547.
(9) Watanabe, H. In *Structure and Properties of Multiphase Polymeric Materials*; Araki, T., Tran-Cong, Q., Shibayama, M., Eds.; Marcel Dekker: New York, 1998; pp 317−360.
(10) Fujimura, M.; Hashimoto, T.; Kawai, H. *Rubber Chem. Technol.* **1978**, *51*, 215.
(11) Panyukov, S.; Rubinstein, M. *Macromolecules* **1996**, *29*, 8220.
(12) Sakurai, S.; Iwane, K.; Nomura, S. *Macromolecules* **1993**, *26*, 5479.

(13) Sakurai, S.; Aida, S.; Nomura, S. *Polymer* **1999**, *40*, 2071.
(14) Hashimoto, T.; Nagatoshi, K.; Todo, A.; Hasegawa, H.; Kawai, H. *Macromolecules* **1974**, *7*, 364.
(15) Sakurai, S.; Momii, T.; Taie, K.; Shibayama, M.; Nomura, S.; Hashimoto, T. *Macromolecules* **1993**, *26*, 485. In the course of solvent evaporation, the lamellar microdomains formed in the cast solution preferentially orient parallel to the surfaces. The domain structures are frozen-in when the PS lamellae are vitrified. Since the PS lamellae still contain a certain amount of the solvent, contraction takes place during successive evaporation of the solvent. In this process, the thickness of the cast solution keeps decreasing with keeping its area constant. As a result, the lamellae oriented parallel to the surfaces are compressed. The lamellae oriented perpendicularly to the surfaces are not affected by such an effect.
(16) Sakurai, S.; Sakamoto, J.; Shibayama, M.; Nomura, S. *Macromolecules* **1993**, *26*, 3351.

MA002123+